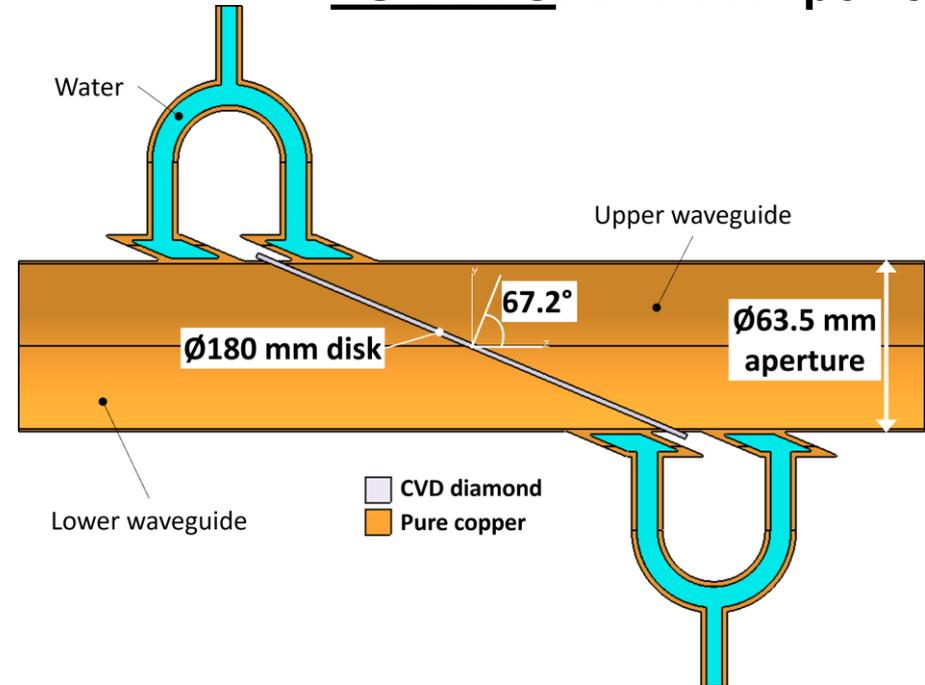# Diamond windows for microwave application: numerical analyses and characterization by microscope and Raman measurements

**G. Aiello**, A. Meier, T. Scherer, S. Schreck, D. Strauss

Context

- Electron cyclotron heating and current drive (EC H&CD) system in nuclear fusion devices

- Diamond Brewster-angle window as smart broadband solution

- Gyrotron frequency step-tunability in 2-3 GHz over a range of ±10 GHz at main frequencies of interest (e.g., 170/204 GHz)

- Technological limits (Ø140 mm) pushed towards **Ø180 mm** diamond disks

EU DEMO: 2 MW RF power

Water

Upper waveguide

67.2°

Ø180 mm disk

Ø63.5 mm aperture

Lower waveguide

☐ CVD diamond
■ Pure copper

Outline

- Numerical analyses to check performance of the Brewster-angle window with large disk at the given thickness
  - no constant tanδ input, but input with tanδ mapping
- Characterization of the large disk by microscopy and Raman for microfeatures and residual stresses

(µm)
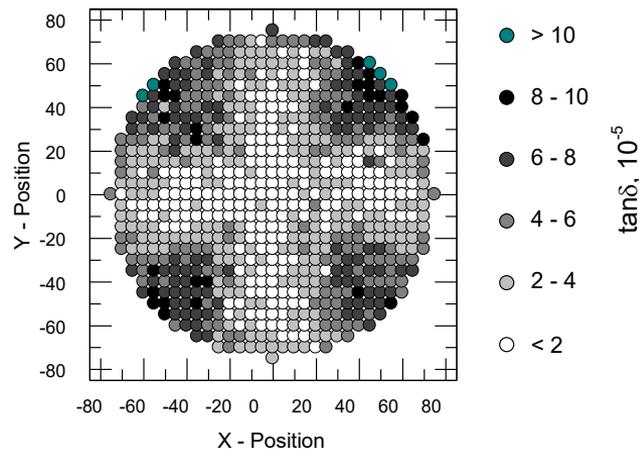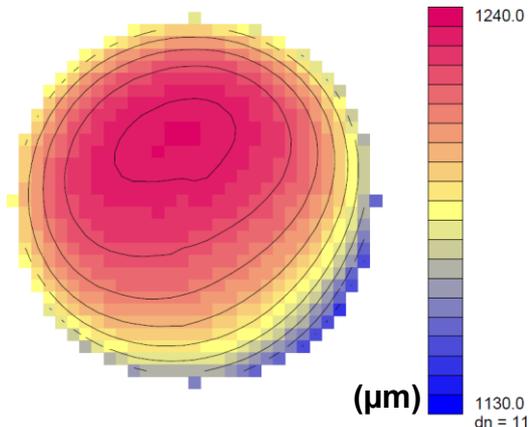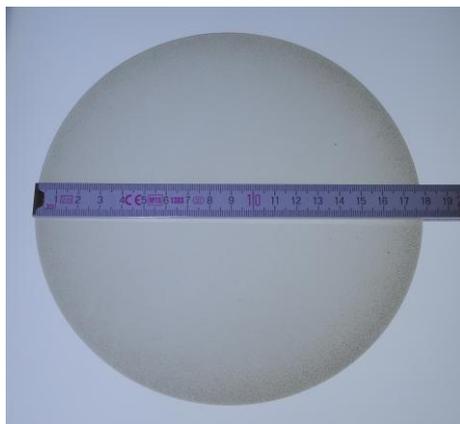
- Manufactured by DM, Freiburg
- ~1230 µm thick at center, in the range 1100 – 1150 µm at disk edge
- Loss tangent (tanδ) mapping on the disk

Numerical analyses
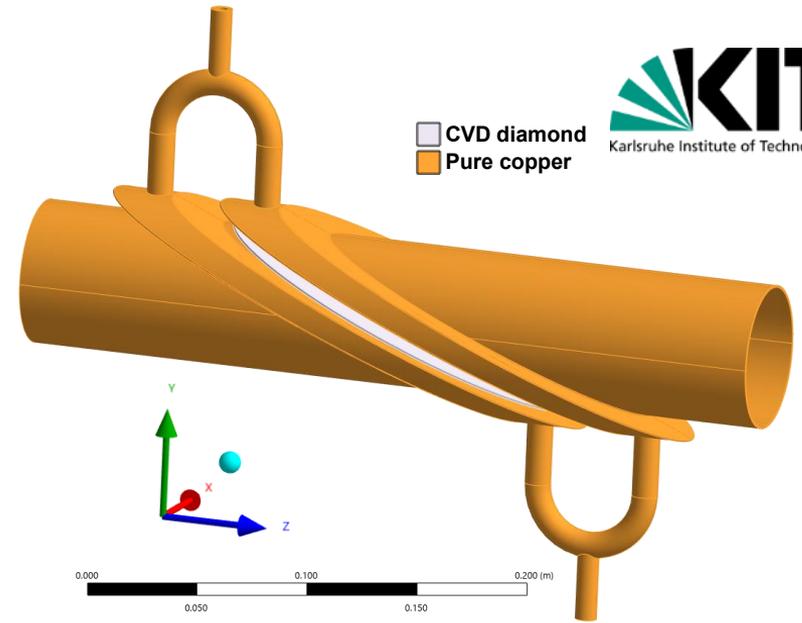
- Thermal, structural analyses
- Entire model of the window (no symmetry)
- Diamond disk with 1.1 mm thickness (lower bound value), 180 mm major axis and 95 mm minor axis
- Beam scenario: 2 MW @ 204 GHz
- HE_{11} mode beam on torus side (NO, overpressure)
- NO includes thermal loads, coolant pressure and gravity
- tanδ mapping input by dedicated macro

CVD diamond
Pure copper

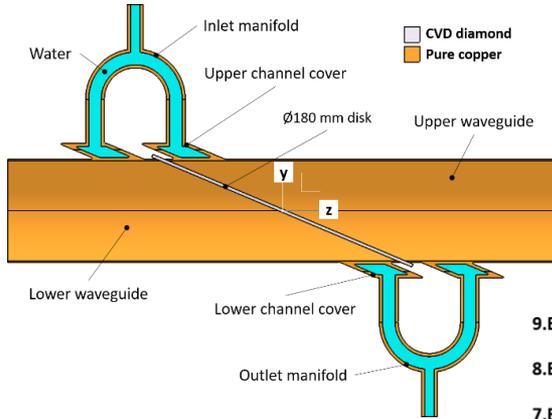| N	dN @ 170 GHz (mm)	dN @ 204 GHz (mm)	dN @ 238 GHz (mm)
1	0.402	0.335	0.287
2	0.803	0.669	0.574
3	**1.205**	**1.004**	0.861
4	1.607	1.339	**1.148**
5	**2.008**	1.673	1.434
6	2.410	**2.008**	1.721
7	2.811	2.343	**2.008**

Different thickness values close to 1.1 mm to minimize the orthogonal polarization at the frequencies of interest

$$d_N = N \cdot \frac{c_0}{2f} \cdot \frac{\sqrt{\varepsilon_r'+1}}{\varepsilon_r'}$$

*M. Thumm et al., FED **53** (2001) 407-421*

Single value tanδ input in the disk - 2023

1. CFD conjugated heat transfer analysis
2. Structural analysis

- 2 MW @ 204 GHz
- Beam radius w_0 = 15 mm
- Disk thickness t = 2 mm
- tanδ = 3.5 x 10^{-5} (P_{abs} = 1546 W)
- 12 l/min and 20°C at inlet
- 0 Pa at outlet
- Heat generation load applied to disk as volumetric power density along radius according to a Gaussian beam, in this example
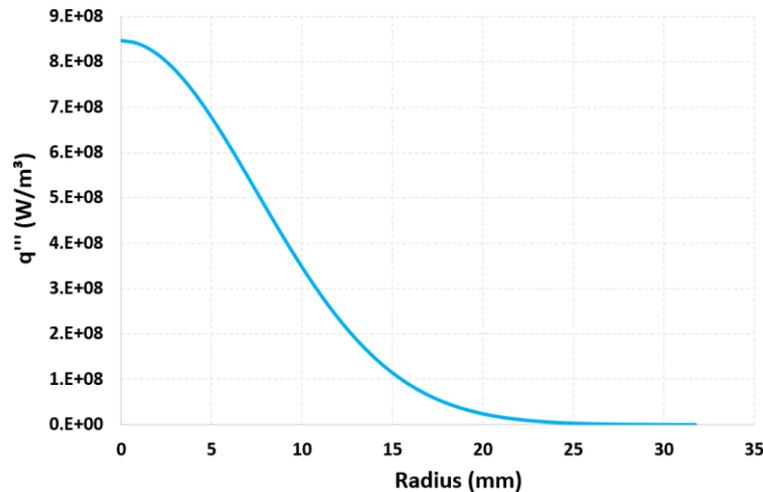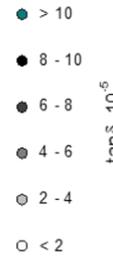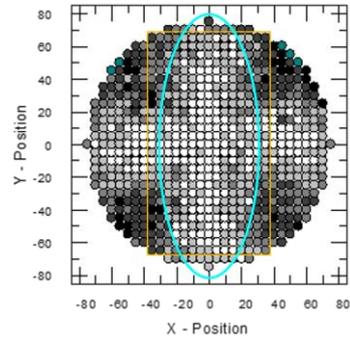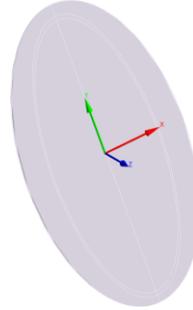
$$P_{abs} = \frac{P_{beam} \, 2 \, \pi \, \nu \, \sqrt{\varepsilon_r} \, tan\delta \, t}{c \, \sin(\theta_B)}$$

$$q'''(r) = \frac{2 \, P_{abs}}{k \, \pi \, w_0^2 \, t} e^{-2\frac{r^2}{w_0^2}}$$

Mapping tanδ input – HE$_{11}$ mode

tanδ mapping
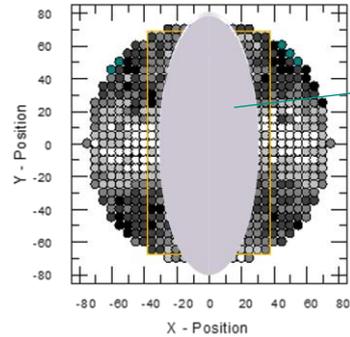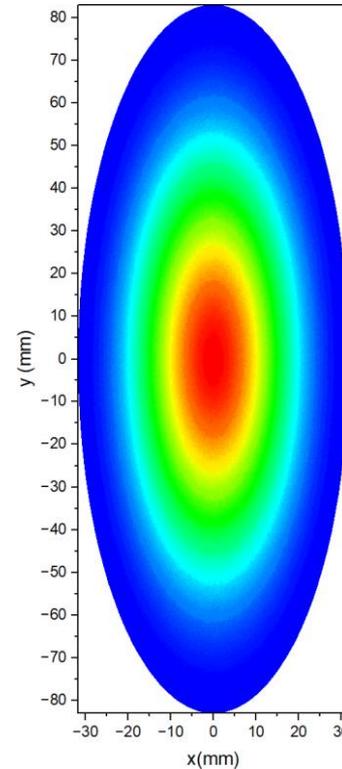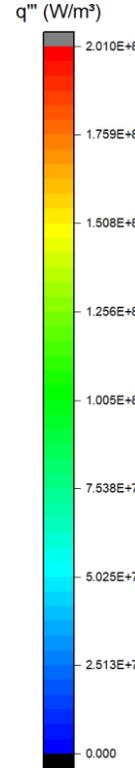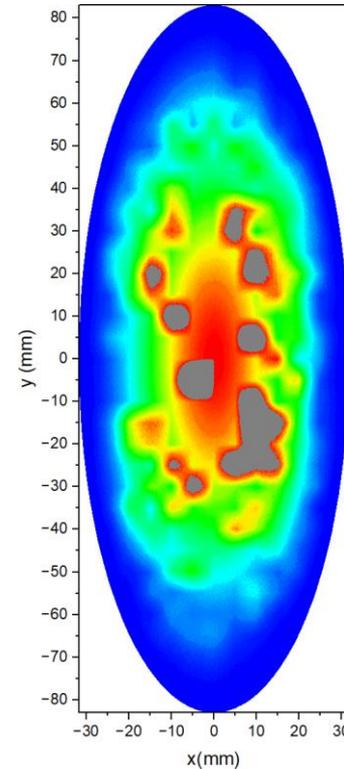
Region of the disk faced by the beam

- tanδ values from mapping are used to calculate the P_{abs} in each mesh element of the disk

- More realistic picture of the window performance

- Comparison done for *HE$_{11}$ mode* beam by thermal and structural analyses with two tanδ values: 2×10^{-5} and 3×10^{-5}
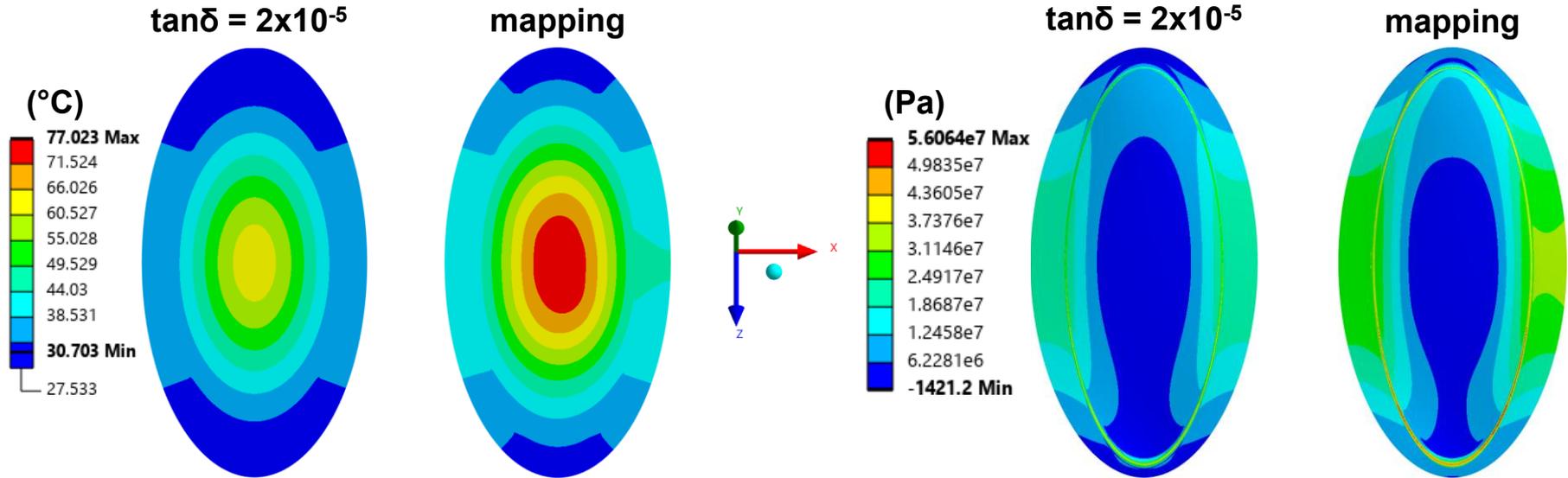
q''' (W/m³)

tanδ = 2×10^{-5}   **mapping**

Comparison 2x10⁻⁵ – mapping

- Thermal analysis with water at 20°C, $h = 5000$ W m⁻² °C⁻¹ (average from CFD analysis)
- Structural analysis with only thermal loads
- $P_{abs} = 486$ W by $\tan\delta = 2\times10^{-5}$, $P_{abs} = 670$ W by mapping (**184 W** difference)
- Max T and stress lower of ~13°C and ~14 MPa by $\tan\delta = 2\times10^{-5}$, different distribution

Comparison 3x10⁻⁵ – mapping
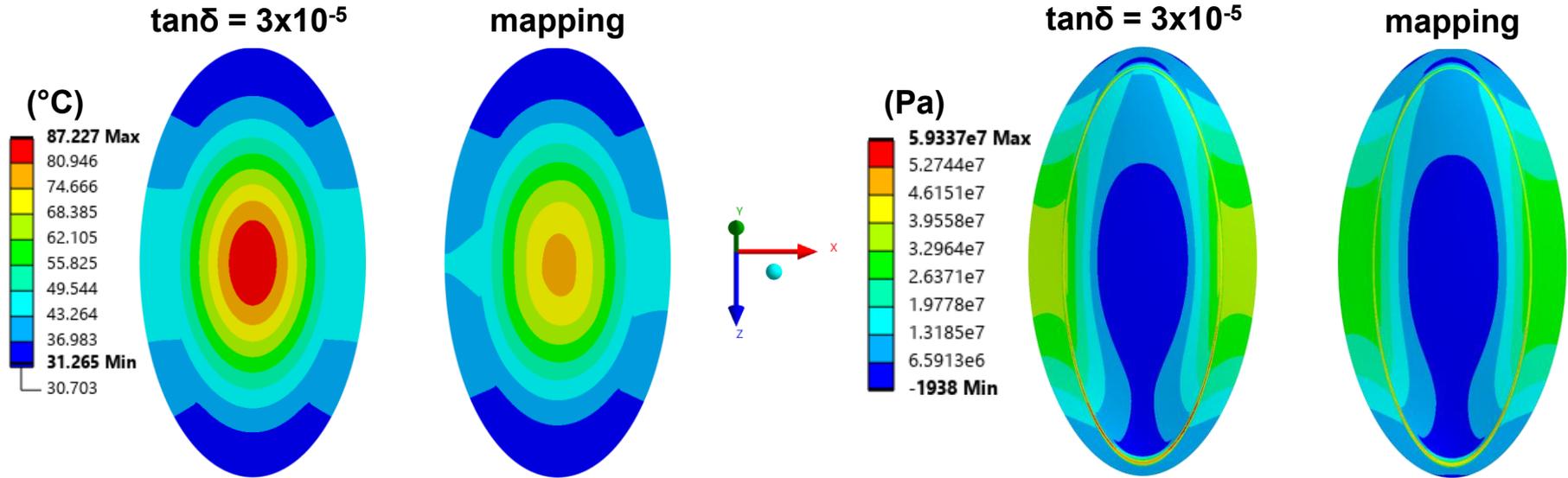
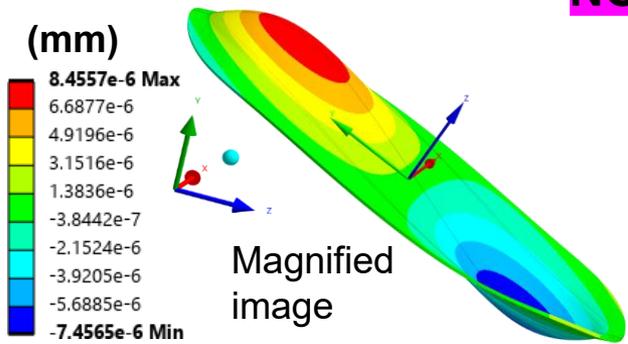$\tan\delta = 3\times10^{-5}$ mapping (°C)

$\tan\delta = 3\times10^{-5}$ mapping (Pa)

- Thermal analysis with water at 20°C, h = 5000 W m⁻² °C⁻¹ (average from CFD analysis)
- Structural analysis with only thermal loads
- P_{abs} = 729 W by $\tan\delta = 3\times10^{-5}$, P_{abs} = 670 W by mapping (**59 W** difference)
- Max T and stress greater of ~10°C and ~3 MPa by $\tan\delta = 3\times10^{-5}$, different distribution

Design verification, mapping + 1x10⁻⁵ (I)
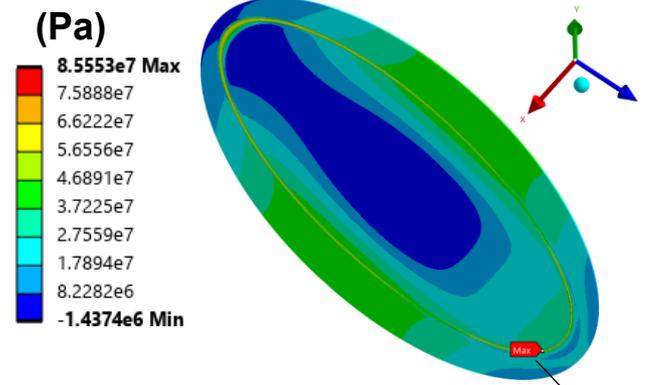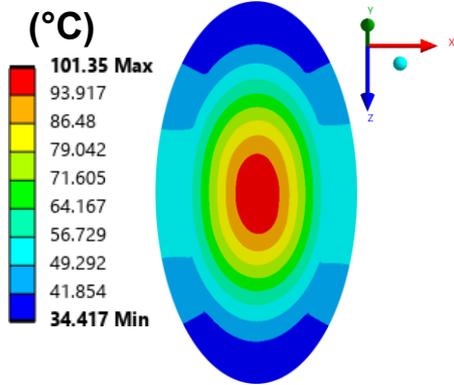
(°C)

101.35 Max
93.917
86.48
79.042
71.605
64.167
56.729
49.292
41.854
34.417 Min

(Pa)

8.5553e7 Max
7.5888e7
6.6222e7
5.6556e7
4.6891e7
3.7225e7
2.7559e7
1.7894e7
8.2282e6
-1.4374e6 Min

NO

~85 MPa, confirmed by submodeling

(mm)

8.4557e-6 Max
6.6877e-6
4.9196e-6
3.1516e-6
1.3836e-6
-3.8442e-7
-2.1524e-6
-3.9205e-6
-5.6885e-6
-7.4565e-6 Min

Magnified image

- P_{abs} = 913 W
- Water at 20°C
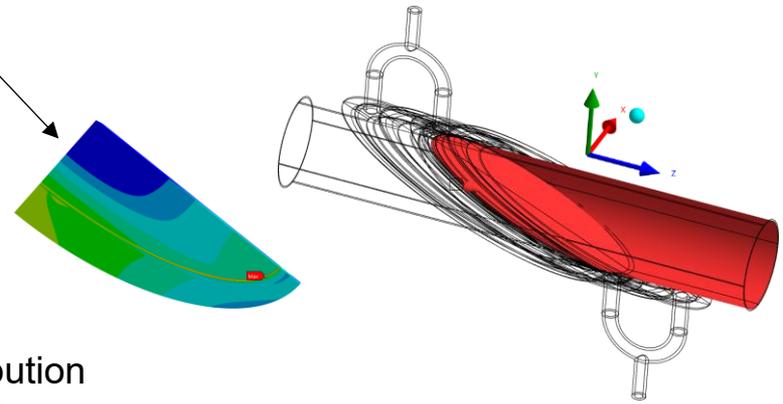- As expected, anti-symmetrical distribution of stress and deformation

- tanδ mapping is used for a better picture of the window performance
- 1x10⁻⁵ is added to the mapping as safety margin against potential tanδ degradation
- **NO** (thermal loads, gravity, 10 bar coolant pressure)
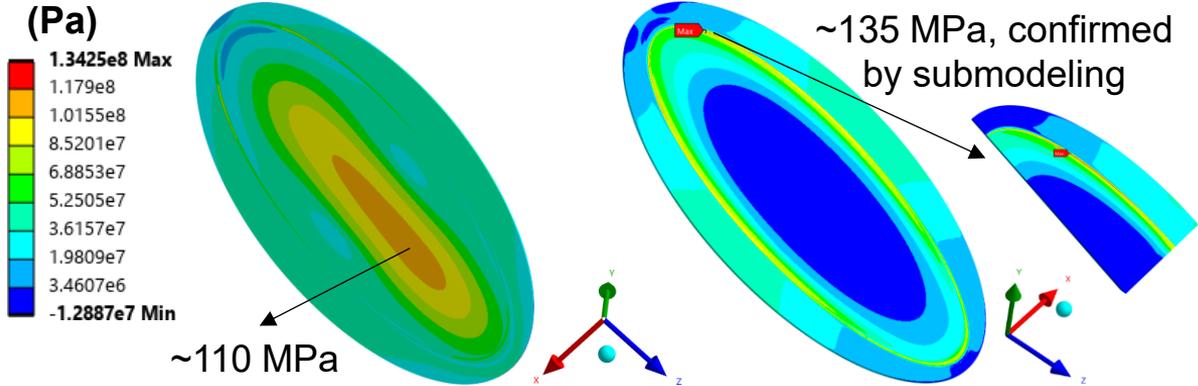- **NO + 1 bar** overpressure

Design verification, mapping + 1x10⁻⁵ (II)

(Pa)

1.3425e8 Max
1.179e8
1.0155e8
8.5201e7
6.8853e7
5.2505e7
3.6157e7
1.9809e7
3.4607e6
-1.2887e7 Min

~110 MPa

~135 MPa, confirmed by submodeling

(mm)

3.3548e-5 Max
2.21e-5
1.0651e-5
-7.9698e-7
-1.2245e-5
-2.3693e-5
-3.5142e-5
-4.659e-5
-5.8038e-5
-6.9486e-5 Min

Magnified image

- tanδ mapping is used for a better picture of the window performance
- 1x10⁻⁵ is added to the mapping as safety margin against potential tanδ degradation
- **NO** (thermal loads, gravity, 10 bar coolant pressure)
- **NO + 1 bar** overpressure
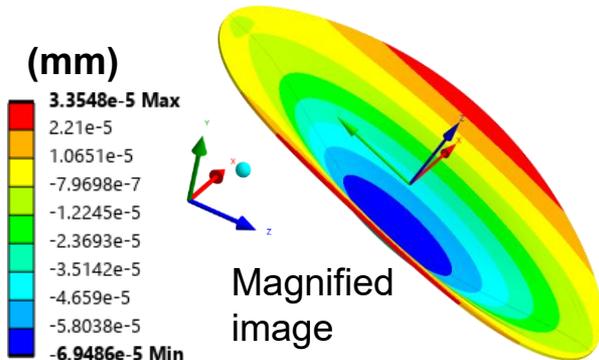
- Bow ~ 70 µm
- Max stress ~135 MPa, lower than limit (150 MPa)
- Window design is verified within these assumptions, 1.1 mm & 180 mm disk
- Stress at tensile side > 200 MPa by 2 bar overpressure

NO + 1 bar
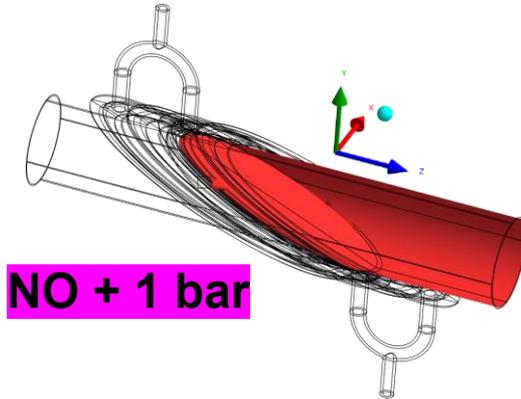
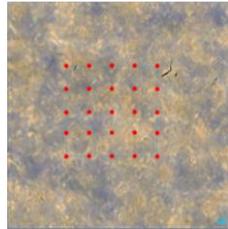# Characterization, 180 mm large disk – Raman (I)

- LabRam HR Evolution Raman Spectrometer
- Characteristic diamond Raman band at 1332 cm^{-1} in stress-free conditions
- Residual stresses cause shift of the Raman peak
- $v_s - v_r = \alpha\,\sigma$
  - v_s, measured frequency of Raman peak (cm^{-1})
  - v_r, frequency of stress-free material (cm^{-1})
  - α, coeff. of stress-induced frequency shift (cm^{-1} GPa^{-1})
  - σ, stress (GPa)
- Shift of the Raman peak position was measured along 2 lines on GS and NS of the disk
  - In each line, regions of ~2 mm x 2 mm were defined *at same time* from disk center to edge at 10 mm step
  - In each region, Raman mapping measurements were carried out in a square grid of 1 mm x 1 mm containing 25 points
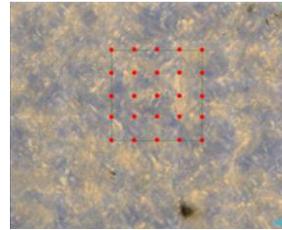
90° line

0° line

Ø180 mm, GS
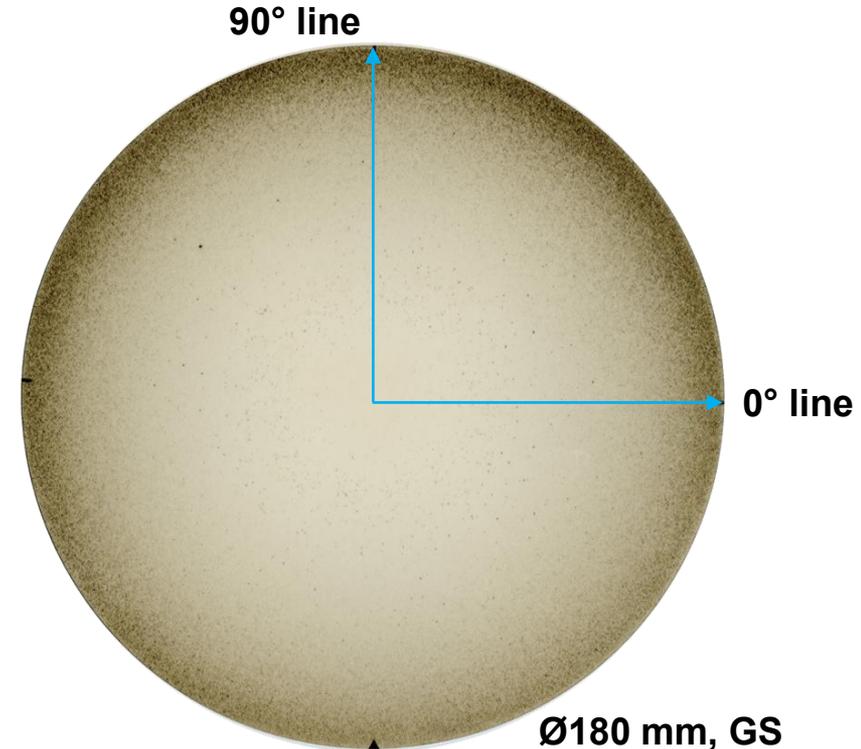
Characterization, 180 mm large disk – Raman (II)

- 532 nm, 25% power, 1800 g/mm, x10, 50μm aperture
- 3 times acquisition of 1s in each of 25 points in the range 1200 – 1500 cm^{-1}
- Average spectrum from the grid in each region
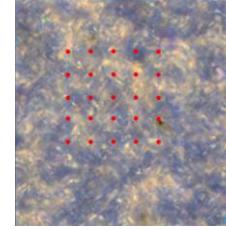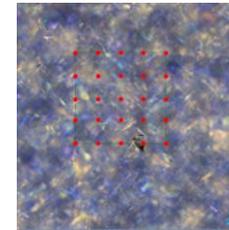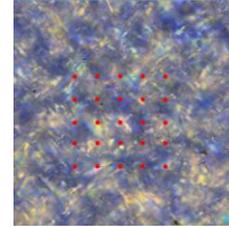- Lorentz fitting to obtain the Raman shift

r = 0 mm   **r = 10 mm**   **r = 20 mm**   **r = 30 mm**   **r = 40 mm**
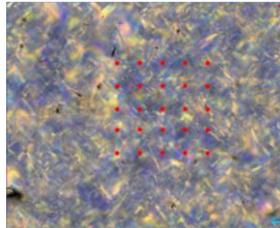
r = 50 mm   **r = 60 mm**   **r = 70 mm**   **r = 80 mm**   **r = 88 mm**

90° line

0° line

Ø180 mm, GS
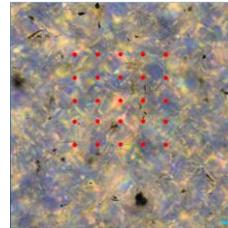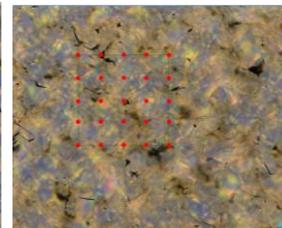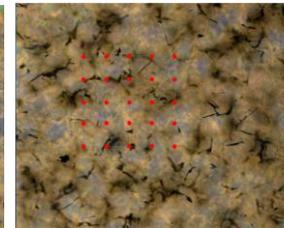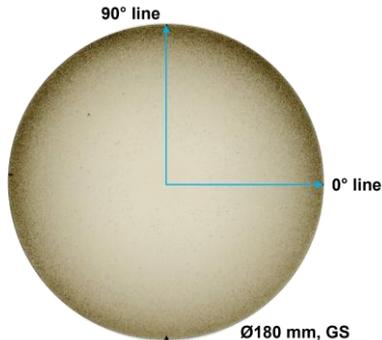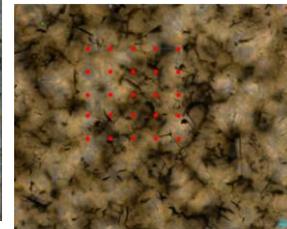
Regions and related maps in the **GS 0° line**

Characterization, 180 mm large disk – Raman (III)

- Raman band shift:
  $$\nu_s - \nu_r = \alpha\,\sigma$$
  with $\nu_r = 1332\ \mathrm{cm}^{-1}$

- Residual stress decreases monotonically from center to edge of the disk

- Shift to lower frequencies relates to tensile stresses

- Max shift of ~0.8 cm^{-1} on NS and ~0.6 cm^{-1} on GS

- On NS, difference of the shift between disk center and edge is ~0.8 cm^{-1}

- On GS, difference of the shift between disk center and edge is ~0.5 cm^{-1}


Ø180 mm, GS
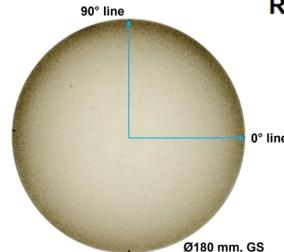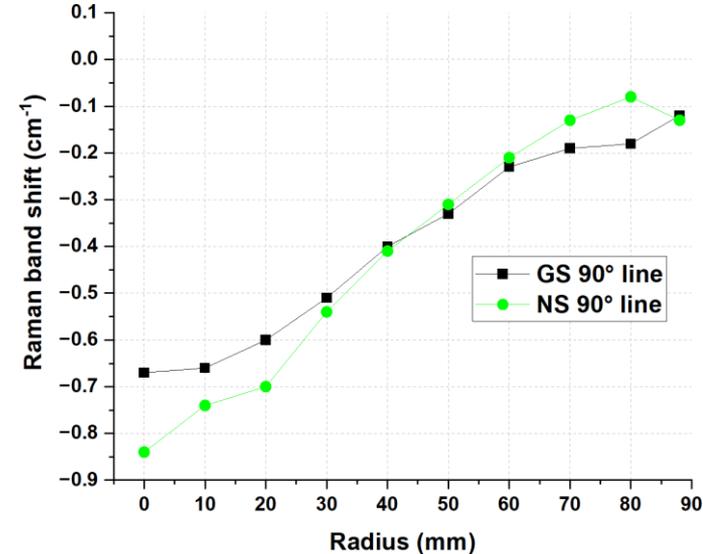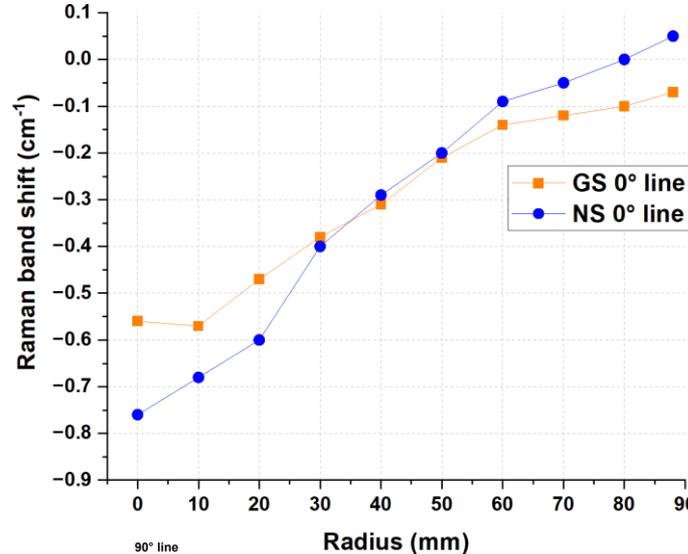
<u>Further investigations</u> to run with more measurement points and lines, different objectives (surface and bulk contributions) and laser wavelengths
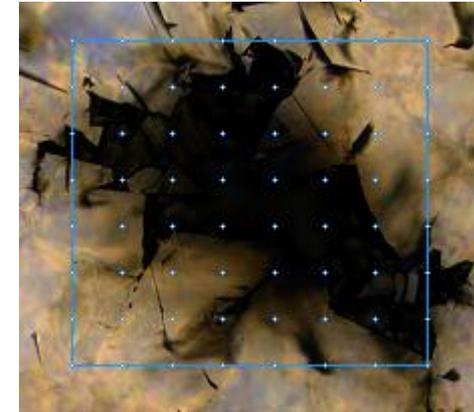
Microfeatures, 180 mm large disk – Raman

- Initial investigation of some relevant dark microfeatures by microscope and Raman mapping
- Graphite appears in microfeature #1 and #3
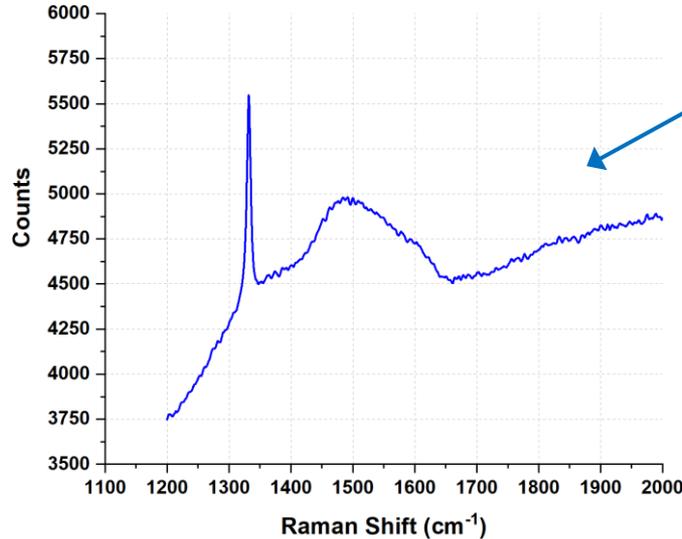- Work to continue by different combination of parameters

532 nm,
25% power,
1800 g/mm,
x10 objective,
50μm aperture,
30s acquisition,
2 times

Ø180 mm, GS
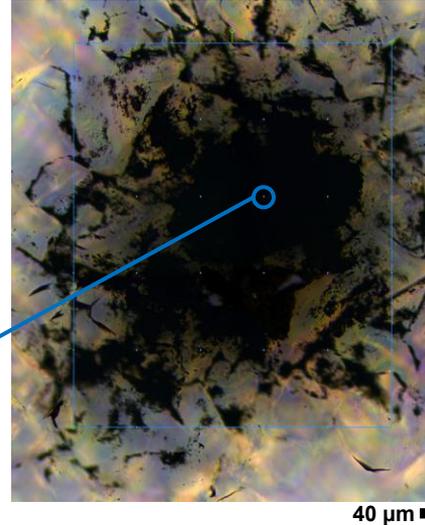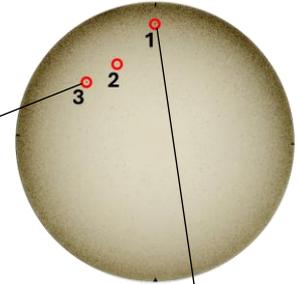
40 μm

Microfeatures:

#1 at r ~ 76 mm

#2 at r ~ 50 mm

#3 at r ~ 58 mm

100 μm

1520 to 1610 cm^{-1}, Raman G-band,
A.M. Zaitsev, Optical properties of diamond: a data handbook, Springer, 2001.

IAM - AWP

Summary and outlook

- Window design with the manufactured 1.1 mm & 180 mm diamond disk was verified

- Raman mapping has been introduced for residual stress measurement and differences are observed between center and edge of the large disk

- Graphite appears in some microfeatures by Raman measurements

- Raman measurements shall be continued also in collaboration with high resolution tanδ measurements, especially at locations featuring high density of microfeatures